Cell Proliferation

Cell Prolif., 2011, **44**, 537–549 doi: 10.1111/j.1365-2184.2011.00788.x

Chitosan enhances mineralization during osteoblast differentiation of human bone marrow-derived mesenchymal stem cells, by upregulating the associated genes

S. Mathews*, P. K. Gupta*, R. Bhonde* & S. Totey†

**Manipal Institute of Regenerative Medicine, Manipal University, Domlur, Bangalore, India and †Kasiak Research Pvt. Ltd., Makers Chamber VI, Nariman Point, Mumbai, India*

Received 9 *June* 2011*; revision accepted* 20 *August* 2011

Abstract

Objectives: Chitosan is widely used as a scaffold for bone tissue engineering. However, up-to-date, no previous detailed study has been conducted to elucidate any mechanism of osteogenesis by chitosan itself. Here, we have evaluated effects of chitosan-coated tissue culture plates on adhesion and osteoblast differentiation processes of human mesenchymal stem cells (hMSCs), isolated from adult bone marrow.

Materials and methods: Tissue culture plates coated with chitosan at different coating densities were used to evaluate the effects on hMSC adhesion and osteoblast differentiation. hMSCs were induced to differentiate into osteoblasts on the chitosan-coated plates and were evaluated using established techniques: alkaline phosphatase assay, demonstration of presence of calcium and real time PCR.

Results: The cells adhered to plates of lower coating density of chitosan, but formed viable cell aggregates at higher coating density (100 μg/sq.cm). Coating density of 25 μg/sq.cm, supporting cell adhesion was chosen for osteoblast differentiation experiments. Differentiating hMSCs showed higher mineral deposition and calcium content on chitosan-coated plates. Chitosan upregulated genes associated with calcium binding and mineralization such as collagen type 1 alpha 1, integrin-binding sialoprotein, osteopontin, osteonectin and osteocalcin, significantly.

Conclusions: We demonstrate for the first time that chitosan enhanced mineralization by upregulating the associated genes. Thus, the study may help clinical situations promoting use of chitosan in bone mineralization, necessary for healing non-union fractures and more.

Correspondence: S. Totey, Kasiak Research Pvt. Ltd., #31, Makers Chamber VI, Nariman Point, Mumbai-400021, India. Tel.: +91-22-22881097; E-mail: smtotey@gmail.com

Introduction

Every year, an estimated 9 million fracture cases occur globally (1). Currently, autologous bone graft is considered to be the gold standard for augmenting bone regeneration *in situ*. However, limited sourcing, and volume of bone graft, as well as donor site morbidity and related complications, have led to desire for development of alternative treatments to maintain effectiveness, minimize disadvantages and be made affordable to world population (2). Tissue engineering and cell-based therapies have opened up a new era of regenerative medicine, promising replacement or regeneration of no longer-functional or damaged body parts (3,4). One of the most exciting approaches is cell-based bone tissue engineering (BTE), which combines the use of living osteogenic cells with biomaterial scaffolds *ex vivo* to allow development of a three-dimensional tissue construct (5).

With advancement in the field of tissue engineering, significant research has been carried out to identify suitable scaffold materials and cell sources for reconstructing or repairing the tissue of interest (6). Identification of multi-potential mesenchymal stem cells (MSCs) derived from various adult human tissues has provided exciting prospects for cell-based tissue engineering and regeneration (7,8). As MSCs have the potential to differentiate into osteoblasts, they can be explored for development of a bioengineered bone construct using various biomaterial scaffolds (9). The goal is that the cells should attached to the scaffold, then replicate, differentiate and organize into normal healthy tissue, as the scaffold degrades.

While choosing a biomaterial for tissue engineering applications, apart from basic qualities such as biocompatibility and biodegradability, it is important to understand roles of the particular biomaterial in question, in controlling behaviour and fate of the cells of interest (10). Cell–material interactions should be understood in terms of the chemical nature of the material, protein adsorption, cell adhesion, differentiation and gene expression patterns (11). This knowledge will help us tailor scaffolds of our interest, for wide variety of tissue engineering applications.

Chitosan is a natural biomaterial with structural similarity to hyaluronic acid, of the extra-cellular matrix (ECM) (12,13). Although osteogenic properties of chitosan are well established in tissue engineering applications, exact mechanisms are not yet well understood (14,15), and specific details of osteogenic differentiation of human mesenchymal stem cells on two-dimensional chitosan matrices have not been studied in depth so far. In the present investigation, we have utilized chitosan to modify tissue culture plates to understand its effect on adhesion and osteoblast differentiation of human bone marrow-derived mesenchymal stem cells (hMSCs). Two of our major objectives were to evaluate the potential of chitosan for tissue culture plate modification and to understand mechanisms of osteogenesis by chitosan, in terms of gene expression and mineral matrix deposition. These results will pave the way for developing chitosan-based culture plates and biomimetic scaffolds for various cell culture and BTE applications.

Materials and methods

Isolation and characterization of human bone marrow-derived mesenchymal stem cells

Institutional ethics committee approval was taken before initiating the study then hMSCs were isolated and characterized from bone marrow aspirations of adult volunteers, by methods described elsewhere (16). Briefly, hMSCs were isolated using their property of plastic adherence, from the mononuclear fraction of bone marrow obtained by density gradient centrifugation with Lymphoprep ™ (1.077 g/ml; Axis-Shield, Point-of-care division, Oslo, Norway). Cells were cultured in Knockout-DMEM (Gibco, Invitrogen, Carlsbad, USA) medium supplemented with 10% foetal bovine serum (certified Australian, HyClone, Logan, USA), 2 mM L-glutamine (Gibco, Invitrogen) and 1% Pen Strep(10 000 units/ml Penicillin and 10 000 μg/ml Streptomycin; Gibco, Invitrogen). This medium will be referred to as hMSC medium, hereafter. Cells were then characterized by immunophenotyping for expression of hMSC-specific cell surface markers. Here, we characterized them for CD90, CD73, CD44, CD105, CD166, as positive markers and haematopoietic markers such as CD45 and CD34 as negative markers. All these anti-human antibodies were raised in mouse and were obtained from BD Pharmingen (San Jose, CA, USA). Immunophenotyping was carried out by flow cytometry using an LSR-II instrument (BD Biosciences, San Jose, CA, USA) and data were analysed using FACS Diva software (BD Biosciences, San Jose, CA, USA). Cells were also stained for vimentin with anti-human vimentin antibody raised in mouse (BD Pharmingen) and fluorescent images were captured with a Nikon Eclipse 80i microscope (Nikon Corporation, Tokyo, Japan) and analysed by QCapture Pro 6 software (Nikon Corporation, Tokyo, Japan). Nuclei were stained with 4′, 6′-diamidino-2-phenylindole dihydrochloride or DAPI (Sigma-Aldrich, St. Louis, MO, USA). Phase contrast micrographs were obtained on a Nikon Eclipse TE2000-S microscope using QCapture software.

Cells were also tested for their known ability to differentiate into osteogenic and adipogenic lineages by methods mentioned elsewhere (16). Briefly, osteoblast differentiation was induced by growing them in hMSC medium supplemented with 50 μg/ml ascorbic acid, 10 mM β-glycerophosphate and 10^{-8} mM dexamethasone. This medium will be referred to as osteogenic induction medium hereafter. Differentiation into the osteogenic lineage was confirmed by alizarin red S and von Kossa staining for calcium. Adipogenic differentiation was induced by growing the cells in hMSC medium supplemented with 1 μM dexamethasone, 0.5 mM isobutylmethylxanthine, 1 μg/ml insulin and 100 μM indomethacin. Differentiation into adipocytes was confirmed by positive oil red O staining to display oily droplet inclusions.

Plastic laboratory wares such as culture plates, flasks and centrifuge tubes used in the experiments were purchased from BD Biosciences. All osteogenic and adipogenic supplements and reagents were purchased from Sigma-Aldrich.

Preparation of chitosan-coated tissue culture plates

Chitosan powder (>87.61% degree deacetylation, DD), a kind gift from Indian Sea Foods (Cochin, India), was purified by repeated precipitation with 10% NaOH (Merck, Worli, Mumbai, India). Sterile chitosan-coated tissue culture plates were prepared by methods noted elsewhere (17). Briefly, 1% chitosan solution was prepared by autoclaving purified chitosan powder in distilled water and then dissolving it by adding 1 M sterile glacial acetic acid (Merck). Chitosan-coated culture plates were prepared by covering culture plate surfaces with sufficient volume of sterile chitosan solution, at different concentrations. Solutions were then evaporated to dryness at room temperature in a biological laminar flow hood. This resulted in formation of thin chitosan acetate films on plate sur-

faces. Acidity of surfaces was neutralized with 0.1 M NaOH solution. Plates were then washed several times in distilled water until their pH became neutral, then they were dried and stored at 4 °C until use. Plates were equilibrated in Dulbecco's phosphate-buffered saline (DPBS; Gibco, Invitrogen) before use for cell culture experiments and these plates will be referred to as 'chitosan-coated plates' hereafter. Normal tissue culture plates without any coating will be referred to as 'untreated plates'.

Culture of human mesenchymal stem cells on chitosan-coated plates

Bone marrow-derived hMSCs were plated at seeding density of 5000 cells/sq. cm on the chitosan-coated plates prepared at varying concentrations, to optimize coating density that supported cell adhesion and proliferation in hMSC medium. Untreated plates served as controls for these experiments. Plates were scrutinized by phase contrast microscopy for morphological changes and adherence of cells.

Osteoblast differentiation assays on chitosan-coated plates

To evaluate osteogenic potential of chitosan, hMSCs were grown on chitosan-coated plates optimized for hMSC culture. Plates were allowed to reach 90% confluence before initiating differentiation. Cells were directed towards osteogenic lineage by culturing them in osteogenic induction medium. Medium was replenished twice weekly and plates were observed regularly under the phase contrast microscope for mineral deposits. Control plates were incubated in non-osteogenic medium, which is hMSC medium with no additional factors. Plates were removed at specific time periods, days 0, 7, 14 and 21 differentiation, for more specific tests – RNA isolation, histochemical staining, quantification of alkaline phosphatase (ALP) and calcium deposits.

BCIP/NBT staining for alkaline phosphatase

Reagent 5-bromo-4-chloro-3-indolyl phosphate (BCIP)/nitro blue tetrazolium (NBT) was purchased from Sigma-Aldrich and staining was performed according to the manufacturer's instructions. Briefly, medium was aspirated completely and plates were washed three times in DPBS. BCIP/NBT pre-mixed solution was added to the plates and incubated at 37 °C under identical culture conditions, for 30 min. Plates were then observed by phase contrast microscopy for cells stained bluish- or brownish-black.

Alizarin red S and von Kossa staining for calcium

Alizarin red S and von Kossa staining for calcium were carried out on days 7, 14 and 21 differentiation. Briefly, after removing medium completely, cells were fixed in neutral buffered 10% formalin solution (Sigma-Aldrich). Formalin was removed and plates were washed three times in distilled water. For alizarin red S staining, 1% alizarin red S stain was added to the plates and incubated for 10–15 min at room temperature. For von Kossa staining, fixed cells were covered with freshly prepared 5% silver nitrate solution and were exposed to ultra-violet (UV) light for one hour. After removing the stain and washing the plates in water, they were observed using phase contrast microscopy (Nikon Eclipse TE2000-S); images were captured using QCapture Pro 6 software. Gross view photographs were taken using a Nikon D3000 digital camera.

Alkaline phosphatase assay

ALP assay was performed on days 7, 14 and 21 differentiation by methods mentioned elsewhere (18). Briefly, cells were harvested by 0.25% trypsin-EDTA (Gibco, Invitrogen) and total protein was extracted using 1% Triton X (Sigma-Aldrich). Extracted protein was stored at −80 °C until use. The assay was performed by adding 100 µl of each *p*-nitrophenol (*p*-NP) standard and 50 µl of thawed test sample, to 96-well microtitre plates and 50 µl of AMP-substrate buffer containing *p*-nitrophenyl phosphate (*p*-NPP) was then added to each of the test samples. After incubation at 37 °C, absorbance was measured at 405 nm at 5 min intervals for 30 min using a spectrophotometric plate reader (VICTOR 3^{TM} Multilabel Counter, model 1420–032; Perkin Elmer, Cambridge, MA, USA). A standard curve of absorbance versus *p*-NP concentration was generated and used to determine concentration of *p*-NP formed in test samples in mM. Total protein in cell lysate was estimated using the Bradford assay (Sigma-Aldrich). Amounts of ALP present were then normalized to amounts of total protein present. All ALP assay reagents were purchased from Sigma-Aldrich.

Calcium quantification

Plates were removed for calcium quantification on day 21 differentiation. Amounts of calcium in the secreted mineral matrix of osteoblasts was quantified by methods described elsewhere (19). Briefly, after complete medium aspiration, cells were decalcified with 0.6 N HCl (Merck) for 24 h. Amounts of calcium present in HCl supernatant were measured using the *o*-cresolphthalein complexone method (Sigma-Aldrich). Decalcified cells were washed three times in DPBS and solubilized with 0.1 N NaOH/0.1% SDS (Sigma-Aldrich), for total protein extraction. Total protein content was estimated using the Bradford assay. Amounts of calcium measured in the

extracellular matrix were normalized to total protein content of the cells.

Real time PCR for gene expression level analysis of osteoblast differentiation markers

Total RNA was isolated from cells collected on 0, 7, 14 and 21 days differentiation using TRI reagent (Sigma-Aldrich) according to the manufacturer's instructions. RNA was quantified using NanoDrop spectrophotometry (NanoDrop Technologies Inc., Wilmington, DE, USA) and 1 μg of RNA was used for preparation of cDNA, carried out in thermo cycler Veriti (Applied Biosystems, Singapore) using cDNA first strand synthesis kit (Fermentas Inc, Maryland, USA). Quantitative real time PCR was performed in the 7500 Real Time PCR system (Applied Biosystems), using 7500 system SDS (sequence detecting software) software for the specific primers, with Quanti-Fast SYBR Green real time PCR kit (Qiagen, Valencia, CA, USA), according to the manufacturer's instructions. Briefly, the program was set for initial activation at 95 °C for 5 min, followed by 40 cycles of two-step cycling involving a denaturation step at 95 °C for 10 s and combined annealing/extension step at 60 °C for 35 s. Real time PCR analysis was performed for most of osteoblast differentiation-associated genes/proteins: rRunt related-transcription factor 2 (RUNX2), alkaline phosphatase for liver/bone/kidney (ALPL), collagen, type 1, alpha 1 (COL1A1), secreted phosphoprotein 1 (SPP1)/osteopontin(OPN), secreted protein, acidic, cysteine-rich(SPARC)/Osteonectin(ON), Sp7 transcription factor (SP7)/Osterix(OSX), integrin-binding sialoprotein (IBSP) and bone gamma-carboxyglutamate (gla) protein (BGLAP)/Osteocalcin(OCN). Accession number and sequences of all primers used in this experiment are provided in Table 1. All primers used were obtained from Bioneer, Korea. Data were analysed using 7500 system SDS software and cycle threshold or Ct value, correlated with starting quantity of target mRNA, was used for further calculations and analysis of gene expression levels. Ct value for interesting genes was normalized to RN18S1/18S rRNA expression levels. Fold difference in gene expression level of cells grown on chitosan-coated plates with respect to cells on untreated plates was calculated by the formula, fold change = $2^{-\Delta\Delta Ct}$, where ΔCt is difference in Ct values before and after differentiation, and ΔΔCt is the difference in ΔCt values after chitosan coating with respect to untreated plates (20). For quantification of *ALP* gene expression on untreated and chitosan-coated plates at different time points, fold difference was calculated with respect to undifferentiated starting population.

Statistical analysis

Experiments were conducted in triplicate and were repeated with three different donor samples ($n = 3$). Measures for each sample were performed in triplicate and results were expressed as mean ± SD. Statistical analysis was performed using the two-tailed, paired Student's *t*-test. Graphs represent data from a representative donor sample, performed in triplicate. For all analyses, *P*-value <0.05 was considered significant and asterisks are provided accordingly, to indicate levels of significance, $*P < 0.05$, $**P < 0.01$ and $***P < 0.001$.

Results

Characterization of hMSCs isolated from human bone marrow

hMSCs were successfully isolated from adult human bone marrow and characterized by observing culture characteristics, immunophenotyping and differentiation potential (Fig. 1). They were adherent to polystyrene tissue culture-treated plates with spindle shaped fibroblastic morphology (Fig. 1a). Cells were positive for expression of mesenchymal stromal markers CD90, CD73, CD105,

Table 1. The sequences and accession number of the primers used for the real time PCR

GenBank Accession. no.	Gene	Forward primer sequence, 5′–3′	Reverse primer sequence, 5′–3′	Product size, bp
NM_199173.3	BGLAP	GACTGTGACGAGTTGGCTGA	GAAGAGGAAAGAAGGGTGCC	138
NM_001127501.1	ALPL	GAGGTGGCATGAAGCTCAGT	ACCTGCTTTATCCCTGGAGC	162
NM_004348.3	RUNX2	ATTTCTCACCTCCTCAGCCC	CAACAGCCACAAGTTAGCGA	135
NM_001040058.1	SPP1	TCTCCTAGCCCCACAGAATG	GTCAATGGAGTCCTGGCTGT	154
NM_000088.3	COL1A1	CATCTCCCCTTCGTTTTTGA	CCAAATCCGATGTTTCTGCT	109
NM_003118.2	SPARC	GTGCAGAGGAAACCGAAGAG	TCATTGCTGCACACCTTCTC	172
NM_004967.3	IBSP	AACCTACAACCCCACCACAA	AGGTTCCCCGTTCTCACTTT	149
NM_152860.1	SP7	GCCAGAAGCTGTGAAACCTC	GCTGCAAGCTCTCCATAACC	161
NR_003286.2	RN18S1	CGGCTACCACATCCAAGGAAG	AGCTGGAATTACCGCGGCT	188

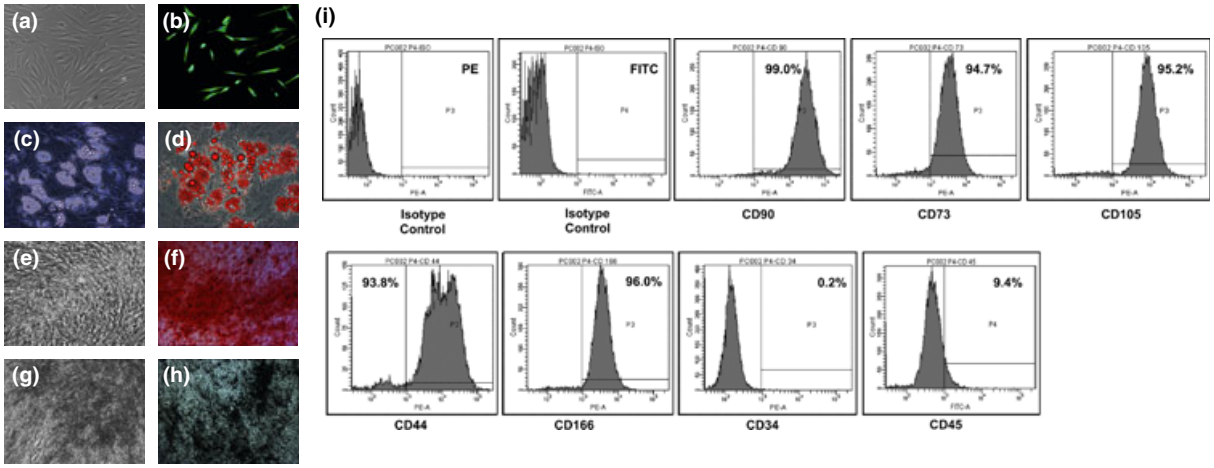

Figure 1. Characterization of adult bone marrow derived human mesenchymal stem cells. (a) Morphology of the cells under phase contrast microscope shows spindle shaped fibroblast like cells. (b) The immunofluorescent micrograph shows the cells stained positive for vimentin. (c) Phase contrast and (d) Oil Red O staining confirmed the differentiation into the adipogenic lineage. (e–h) Differentiation into osteogenic lineage was confirmed by phase contrast and histochemical staining for calcium. (e) Phase contrast micrograph and (f) Alizarin Red S staining on day 14 of differentiation. (g) Phase contrast micrograph and (h) von Kossa staining on day 21 of differentiation. (i) The Immunophenotyping by flow cytometry showed the isolated cells positive for mesenchymal stem cell markers like CD90, CD73, CD105, CD44, CD166 and negative for haematopoetic markers like CD34 and CD45. The total magnification of the micrographs is 100× except (c, d) which is 200×.

CD166 and CD44 and negative for expression of haematopoietic markers CD34 and CD45 (Fig. 1i) and were positive for fibroblast marker, vimentin (Fig. 1b). The cells also differentiated into osteogenic and adipogenic lineages when cultured in respective induction media (Fig. 1c–h). All differentiation experiments were carried out with cells of passage number 4–8 and there was no significant difference in differentiation pattern of cells in this passage range.

Culture of hMSCs on chitosan-coated plates

We used 5, 10, 25, 50 and 100 μg/cm^2 coating density of chitosan in this experiment. On solvent evaporation, chitosan formed a thin film on polystyrene tissue culture plates. hMSCs attached and had fibroblast-like morphology on chitosan plates at coating density 5, 10 and 25 μg/cm^2 (Fig. 2b–d). There was uniform cell distribution on these plates. Coating density of 25 μg chitosan/sq. cm of coat-

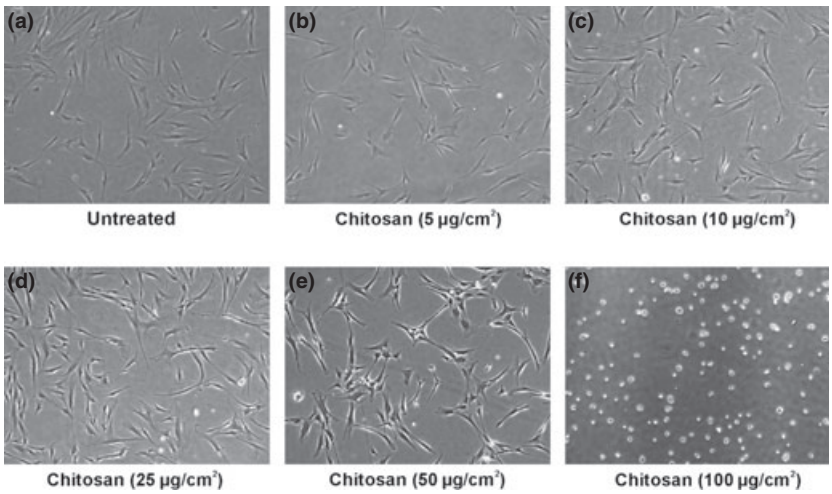

Figure 2. hMSCs culture on tissue culture plates coated with different concentrations of chitosan. (a) Cells on untreated plates. (b–f) Cells on chitosan coated plates. (b–d) hMSCs attached and showed fibroblast like morphology on chitosan plates of coating density 5, 10 and 25 μg/sq. cm. There was uniform cell distribution on these plates. (e) Chitosan plate with a coating density of 50 μg/sq. cm also showed adherent hMSCs but there was non-uniform cell distribution. (f) Chitosan plate with a coating density of 100 μg/sq. cm did not show any adherent hMSCs but there was formation of non-adherent cell aggregates on this plate. A coating density of 25 μg/sq. cm which supported hMSCs adhesion was selected for further osteoblast differentiation experiments. Phase contrast micrographs with a total magnification of 40×.

ing surface was chosen for further differentiation experiments. Chitosan plates with coating density of 50 μg/cm^2 also had adherent hMSCs, but there was non-uniform cell distribution (Fig. 2e). Chitosan plates with coating density of 100 μg/cm^2 had no adherent hMSCs, but there was formation of non-adherent cell aggregates on such plates (Fig. 2f). Re-plating of these aggregates to normal tissue culture plates revealed viable cells, which grew attached to the plates (Fig. 3a,b). When cell aggregates on chitosan-coated plates were maintained in osteogenic induction media for 21 days, they underwent differentiation showing positive alizarin red S staining, for calcium (Fig. 3d).

Evaluation of osteogenic potential of chitosan-coated plates

hMSCs were maintained in osteogenic induction media for a total of 21 days and daily observation under a phase contrast microscope showed presence of mineral deposits after 7–10 days osteogenic induction. There were no marked differences in onset of mineralization of both cells on chitosan-coated and untreated plates. However, there were differences in amounts and patterns of mineral deposition on both types of plate. Mineralization was higher on chitosan-coated plates, which also gave rise to bone nodule formation (Fig. 4). Differentiation was confirmed and compared by histochemical staining and quantified using ALP and calcium assay. Cells maintained in non-osteogenic media showed no mineralization on either type of plate.

ALP staining, assay and gene expression

Alkaline phosphatase is a well-known marker of osteoblast differentiation, and staining for its presence using NBT-BCIP provided indication of differentiation at an early stage. ALP staining performed after 7 days osteogenic induction was used here to compare and analyse expression patterns on chitosan-coated plates with respect to untreated plates (Fig. 5a–d); intensity of staining was higher on chitosan-coated plates (Fig. 5c,d). In the ALP assay, alkaline phosphatase hydrolysed the *p*-nitrophenyl phosphate substrate to furnish the yellow coloured end product *p*-nitrophenol, which was quantified by photometry. ALP assay showed similar patterns of cell expression on both untreated and chitosan-coated plates (Fig. 5e). ALP level increased over the course of differentiation, reaching its peak by the second week, which gradually decreased towards the final phase of mineralization. Level of ALP expression by cells in non-osteogenic medium was very low and there was no significant change in their

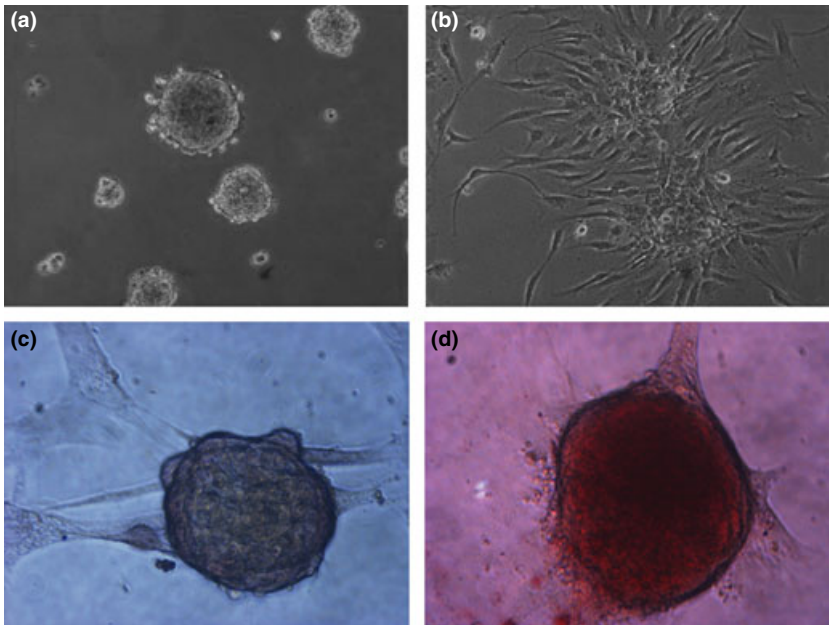

Figure 3. hMSC aggregates on chitosan coated plates. (a) 6 days old cell aggregates on chitosan coated plates (100 μg/sq. cm). (b) The aggregates re-plated into normal tissue culture plates showed attached spindle shaped cells spreading from the aggregates. (c, d) Osteogenic differentiation experiments with the cell aggregates on chitosan coated plates. (c) Alizarin Red S staining for the aggregates in non osteogenic medium for 21 days showed no calcium deposition. (d) Cell aggregates grown in osteogenic media for 21 days gave a positive staining with Alizarin Red S, indicating osteoblast differentiation and mineralization. (a, b) Phase contrast micrographs with a total magnification of 100×. (c, d) Phase contrast micrographs with a total magnification of 400×.

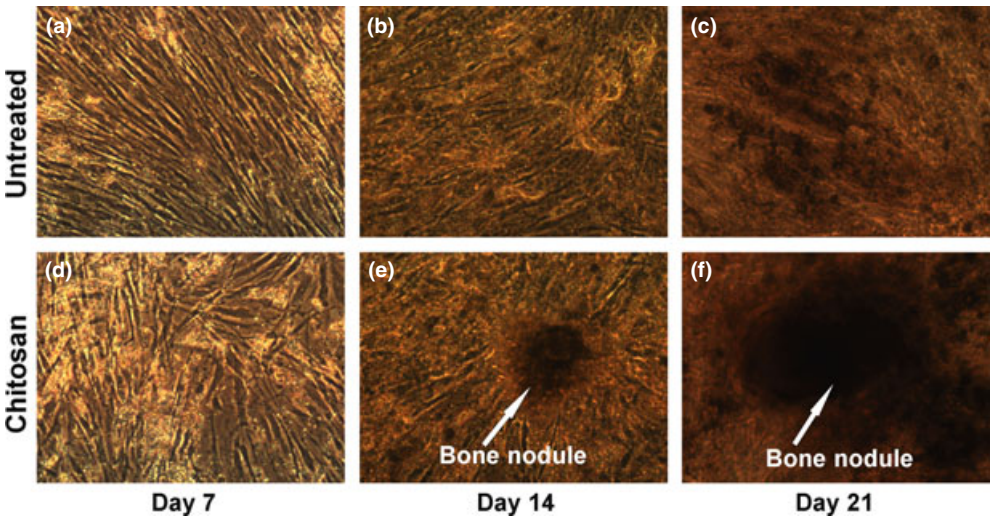

Figure 4. Phase contrast micrographs of cells undergoing osteoblast differentiation on chitosan coated plates. (a–c) Osteoblast differentiation on the untreated plates. (d–f) Osteoblast differentiation on the chitosan coated plates. There were more amounts of mineral deposits by the cells differentiated on chitosan coated plates. (e, f) There was formation of bone nodules by day 14 of differentiation on chitosan coated plates which increased in size by day 21. Total magnification is 100×.

expression level over the entire course of the differentiation experiment.

ALP gene expression analysis for cells undergoing osteoblast differentiation was performed by real time PCR and fold change in expression was calculated with respect to the initial undifferentiated cell population. Results indicated difference in expression patterns on chitosan-coated and untreated plates (Fig. 5f). Cells on untreated plates attained their peak in *ALP* gene expression in the first week of differentiation, which eventually decreased as differentiation progressed and lower levels were maintained during the second and third weeks. On chitosan-coated plates, *ALP* gene expression was low in the first week of differentiation, then increased significantly as differentiation progressed, reaching peaks in expression only by the third week. There was a significant 4-fold increase in *ALP* gene expression by the end of third week osteogenic induction on chitosan-coated plates and this level was twice as high as peak levels on untreated plates. This pattern of expression of ALP at mRNA level did not match the pattern of expression at the protein level.

Alizarin red S and von Kossa staining for calcium

Onset of mineralization was determined by microscope observation of the cells for mineral deposits and was confirmed by alizarin red S staining for calcium. As alizarin red S stains intra-cellular calcium as well as calcium binding proteins and proteoglycans, it was useful in evaluating differentiation at early phases of differentiation. Area and intensity of staining were greater on chitosan-coated plates and intensity increased as the differentiation progressed. Intensely stained patches were observed in cells on chitosan-coated plates compared to those on untreated plates, which had an almost uniform staining pattern (Fig. 6a–d).

Extracellular calcium deposition by mature osteoblasts was confirmed by von Kossa staining, which detected phosphate of calcium phosphate of secreted matrix. Cells undergoing osteoblast differentiation and mineralization provided positive staining, enabling comparison in the third week of differentiation. Here also, intensity of staining was more for mineral deposits on chitosan-coated plates and there were many patches of intense staining (Fig. 6e,f). Cells of both untreated and chitosan-coated plates in non-osteogenic media were negative for alizarin red S and von Kossa staining even after 21 days of culture (data not shown).

Quantification of calcium in mineralized matrix

Quantification of calcium in secreted mineral matrix had 30% increase in calcium deposition when osteogenic induction was carried out on chitosan-coated plates (Fig. 7). This indicated the potential of chitosan to induce bone formation.

Osteoblast differentiation-associated gene expression analysis

To analyse expression of osteoblast differentiation-associated genes, we quantified gene expression of the initial undifferentiated population, and after 7, 14 and 21 days of

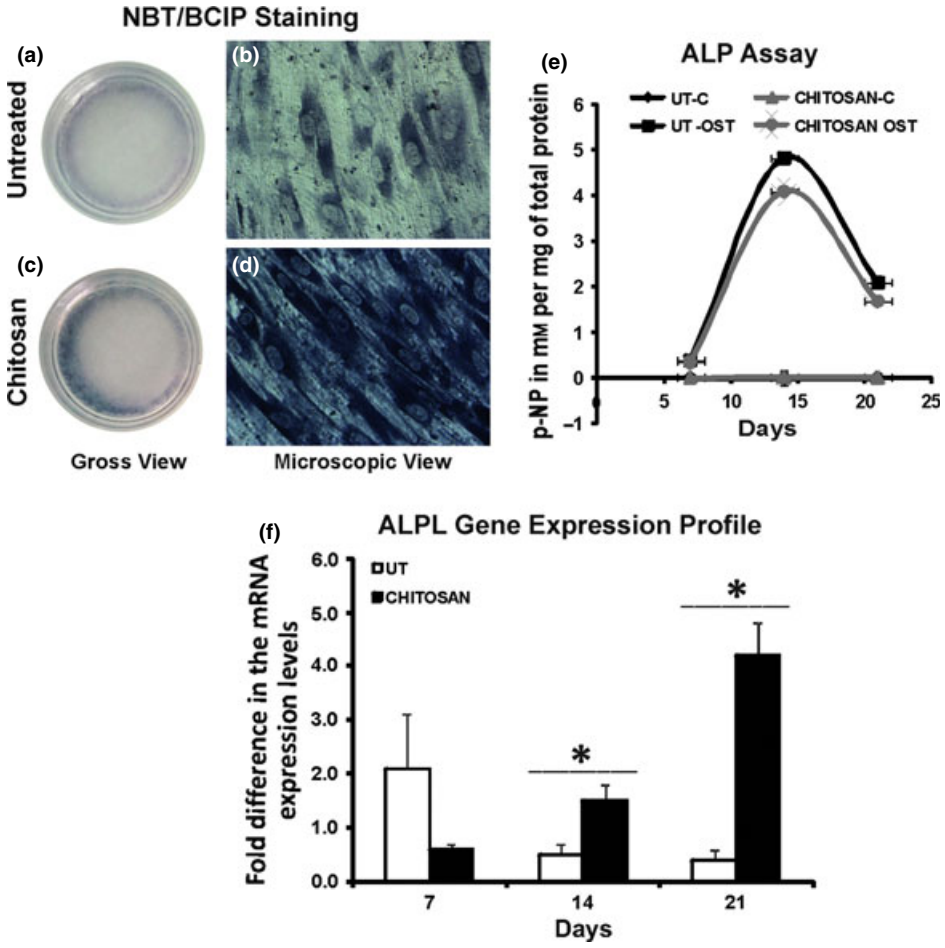

Figure 5. Alkaline phosphatase (ALP) as a marker of osteoblast differentiation. (a–d) Cells undergoing osteoblast differentiation stained for ALP by BCIP–NBT method after 7 days of induction. (a, b) Staining for ALP on untreated plates. (c, d) Staining for ALP on chitosan coated plates. Chitosan coated plates showed more intensely stained cells. (a, c) ALP positive cells were mainly present in the periphery of both the plates (Gross view). (b, d) Phase contrast micrographs with a total magnification of 100×. (e) Alkaline phosphatase assay. The ALP expression pattern was similar on both the untreated (UT) and chitosan coated plates (chitosan). There was significant increase in the ALP expression by the hMSCs in osteogenic induction medium (OST) compared to the hMSCs in non osteogenic medium (C, control). The second week of differentiation showed the peak in ALP expression which is believed to coincide with the initiation of mineralization in both the plates. (f) ALPL mRNA expression levels. mRNA expression levels for ALPL was quantified at different stages of osteoblast differentiation by real time PCR. hMSCs on the UT and chitosan coated plates (chitosan) showed different pattern of expression levels. The peak in ALPL expression was significantly higher on chitosan coated plates (*$P < 0.05$).

osteogenic induction. We evaluated changes in expression levels of eight osteoblast differentiation-associated genes. There was significant fold difference in expression levels of most of these genes by cells on chitosan-coated plates compared to those on untreated plates (Fig. 8). Highest relative fold difference was shown by *OPN*, which indicated 100-fold difference in early phase peaks of cells on chitosan-coated plates. *COL1A1*, a further early marker, showed significant ($P < 0.05$) relative fold difference after 2 weeks induction on chitosan-coated plates. Other mineralization associated genes such as *ON* and *IBSP* also had upregulation in expression on these plates. Relative fold difference in expression level of *OCN*, a final stage and specific osteoblast differentiation marker, gradually increased over the course of differentiation with 5-fold relative difference over the final phase on chitosan-coated plates. *ALPL* had very low relative fold difference on chitosan-coated plates compared to untreated plates in early phases of differentiation, which gradually increased and gave peaks in final phases of mineralization. *RUNX2* displayed only slight increases and its downstream effector *OSX* had marked increase relative expression levels on chitosan-coated plates.

Discussion

In this study, we explored the potential of a natural polymer, chitosan, for its beneficial effect on bone

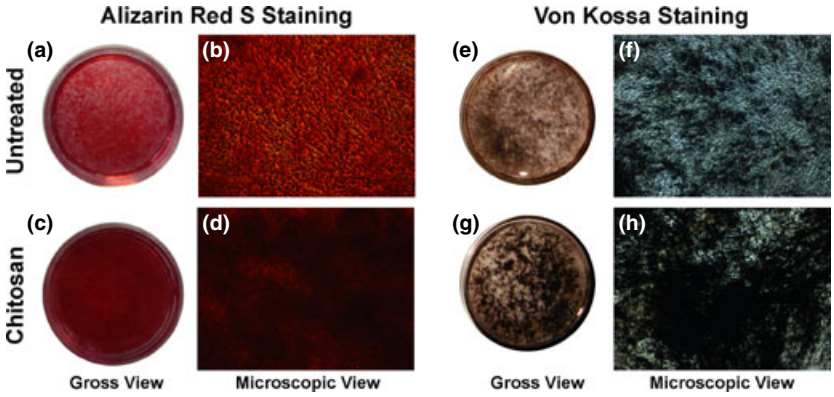

Figure 6. Histochemical staining for calcium. (a–d) Alizarin Red S staining on day 14 of osteogenic differentiation. (a, b) The staining on untreated plate. (c, d) The staining on chitosan coated plates showing more intense staining indicating more calcium deposits or mineralization. (e–h) von Kossa Staining on day 21 of osteogenic differentiation. (e, f) The staining on untreated plate. (g, h) The staining on chitosan coated plate. The Von Kossa staining confirmed the enhancement of mineral matrix deposition by the chitosan coated plates which were evident from the more black deposits on these plates. (b, d, f, h) Phase contrast micrographs with a total magnification of 100×.

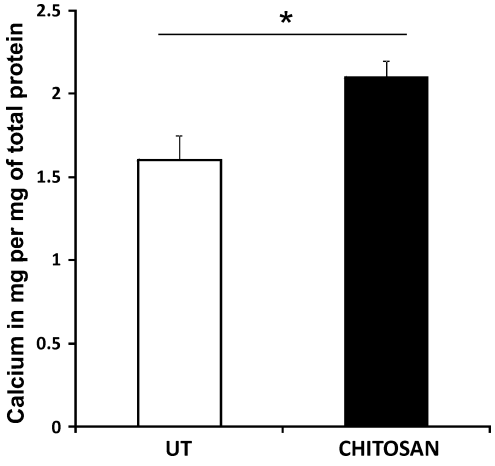

Figure 7. Calcium assay by O-Creolphthalein Complexone method. The amount of calcium in the deposited mineral matrix was quantified on day 21 of osteoblast differentiation and was expressed per mg of total protein. Cells on chitosan coated plates (chitosan) showed significantly high (*$P < 0.05$) calcium deposits compared to the untreated plates (UT).

marrow-derived mesenchymal stem cells' osteogenesis and we examined optimum coating density of chitosan for hMSCs culture. Human MSCs are known for their property of plastic adherence and grow as a fibroblast-like adherent monolayer on tissue culture plates (21,22). Interestingly, we observed formation of viable non-adherent cell aggregates of hMSCs on chitosan-coated plates and observed that such aggregate formation took place at higher coating density of chitosan. Cells of the aggregates were tested to be viable and were able to differentiate into osteogenic lineage. Similar results have been reported with melanocyte culture on chitosan-coated plates (23) when it was hypothesized that melanocyte aggregates on higher concentration of chitosan may be due to changes in cell–chitosan and cell–cell interacting forces.

It is known that hMSCs adhere to biomaterials *via* integrins expressed on their cell surfaces by indirect mechanisms and mediated by specific serum proteins adsorbed to the material surface (24). The type and amount of proteins adsorbed depends on chemical nature of the material (25). One possible explanation for difference in cell adhesion properties of chitosan at different coating density may be due to differences in the adsorbed protein layer on it. This altered protein layer at higher coating density did not allow cells to attach to plates, but instead increased cell–cell interactions resulting in aggregation of the cells. We propose that this property of chitosan can be utilized in cell culture applications, for example, generation of neurospheres and islet-like cell aggregates (ICAs), where non-adherent mesenchymal stem-cell populations are required. Enhanced ICA formation *in vitro* is obtained on non-adherent surfaces (26).

This is a first report on evaluation of osteogenic potential of chitosan, in a two-dimensional culture system. As we used tissue culture plates coated with chitosan, we were able to evaluate osteogenic potential by various parameters such as osteoblast differentiation-associated gene expression levels, calcium quantification, ALP assay and histochemical staining for mineral deposits.

ALP is an early marker and one of the most frequently used markers to demonstrate osteoblast differentiation (27,28). ALP found in bone tissue is called tissue non-specific alkaline phosphatase, which have three isozymes, namely ALP/liver/bone and kidney, abbreviated to ALPL. Although it is a widely used marker, its exact role in osteogenesis has not yet been clear elucidated (29,30).

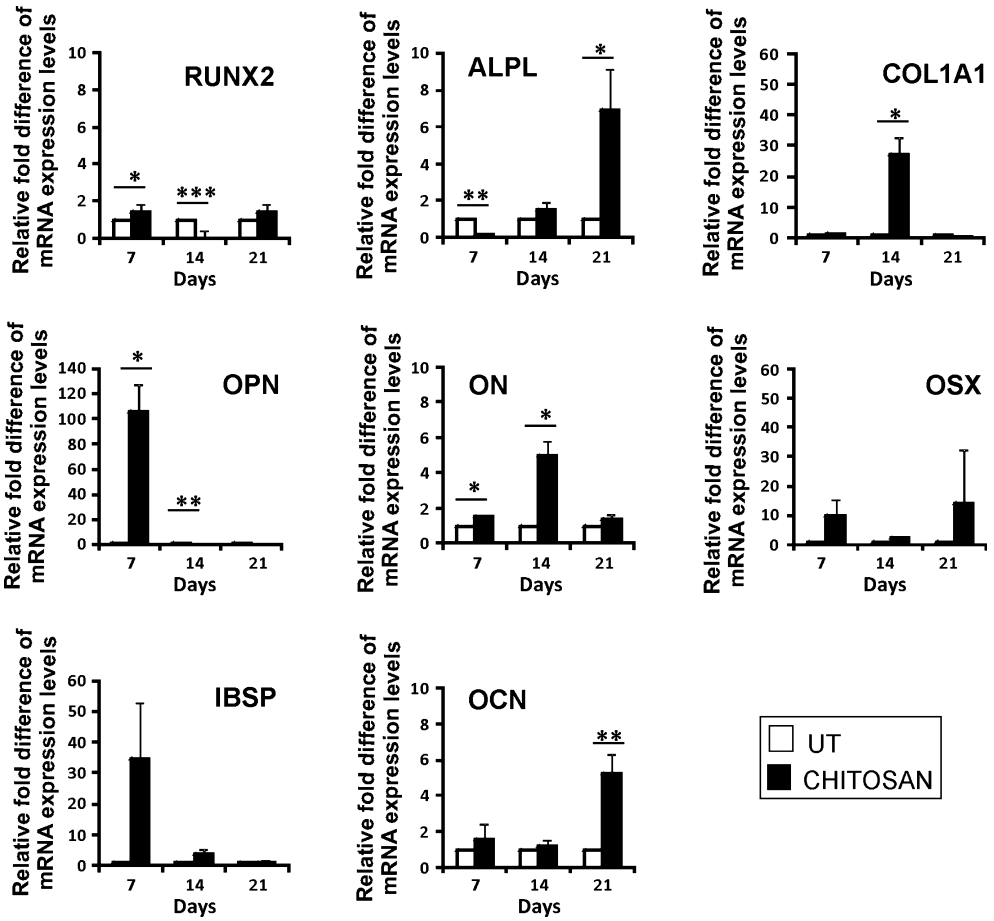

Figure 8. Real time PCR for osteoblast differentiation associated gene expression analysis. The graphs represent the relative fold difference in the gene expression on chitosan coated (chitosan) plates with respect to the untreated (UT) plates. The fold difference was calculated by the $2^{-\Delta\Delta CT}$ method. Cells on chitosan coated plates showed significantly high fold difference in the expression of OPN, IBSP and COL1A1, the three genes regulating respective proteins associated with calcium binding and bone matrix formation. ALPL showed a marked increase and a significantly high expression on day 14 and 21 of differentiation respectively. ON, a later stage and OCN, a final stage differentiation marker also showed significant fold difference on chitosan coated plates. Another key transcription factor OSX, regulating osteoblast differentiation, also showed a marked increase in expression on chitosan coated plates (*$P < 0.05$, **$P < 0.01$ and ***$P < 0.001$).

Evidence suggests that it hydrolyses phosphate substrates releasing P_i and is associated with initiation of mineralization (31). NBT/BCIP staining showed higher numbers of ALP positive cells at the periphery of culture plates, which formed proliferative and hypertrophic zones. In ALP assay, both untreated and chitosan-coated plates had similar patterns of ALP activity, providing peaks at day 14 differentiation. Phase contrast microscopy, as well as histochemical staining, confirmed initiation of mineralization in the second week of differentiation. Interestingly, levels of mRNA expression for ALP on these plates did not provide similar results. Pattern and level of mRNA expression were different for cells on both untreated and chitosan-coated plates. Overall *ALP* gene expression on cells of chitosan-coated plates was 2-fold higher compared to cells differentiated on untreated plates. However, similar results were not observed at the protein level. In their study on effects of alcohol on osteogenic differentiation of hMSCs, Gong *et al.* found that although alcohol significantly reduced alkaline phosphatase activity, there was no effect on alkaline phosphatase mRNA level (32). Perhaps, there is an unknown control mechanism that lies between ALP mRNA expression and its protein level activity.

The final phase of osteoblast differentiation is mineralization, where mineral matrix containing mainly calcium phosphate in the form of hydroxyapatite, is secreted and deposited by mature osteoblasts (33). In our studies, matrix deposition was initiated from the second week of osteoblast differentiation on cells of both untreated and chitosan-coated plates. We used alizarin red S and von

Kossa technique, two widely used staining methods, for analysis of mineral matrix deposition. Alizarin red S staining provided us with early evaluation of osteogenesis, which was confirmed by von Kossa staining at later stages. Both staining methods confirmed marked enhancement of mineralization by cells undergoing osteoblast differentiation on chitosan-coated plates. This finding clearly establishes the well-known osteogenic potential of chitosan scaffolds in a two-dimensional culture system. Chitosan-coated plates showed different yet definite patterns of mineralization as there were more discrete patches with relatively high intensity of staining. One of our experiments even showed formation of bone nodule-like structure by cells only on chitosan-coated plates. This could be due to the higher population of differentiated cells in a particular area, depositing large amounts of calcium in the secreted extracellular matrix. Previous data had shown cell migration/spreading on chitosan or its derivatives (34,35); Fakhry *et al.* reported that chitosan preferentially supported initial adhesion and spreading of osteoblasts over fibroblasts (36). Our data of osteoblast differentiation on chitosan-coated plates demonstrated better mineralization and higher calcium content in the mineral deposits, which are essential for bone healing.

The 'master switch' responsible for initiation of osteoblast differentiation from MSCs is RUNX2, which is also known as osteoblast-specific factor (Osf2) or core binding factor α (Cbfa1) (37,38). Subsequent stages of differentiation can be divided into three phases: proliferative phase, extracellular matrix synthesis and maturation/mineralization phase. Each phase is characterized by expression of specific osteoblast differentiation markers. COL1A1 and OPN appear in the proliferative phase and matrix maturation phase is marked by expression of ALPL, IBSP and COL1A1. The final mineralization phase is distinguished by a second peak in OPN expression and expression of OCN by mature osteoblasts. Collagen, which constitutes around 90% of the organic matrix, is known as the most important marker associated with formation of inorganic matrix of bone (39). It is considered as an early marker of osteoblast differentiation associated with binding of calcium. IBSP is associated with ECM matrix synthesis in the maturation phase and have the potential to act as nucleation points for hydroxyapatite and thereby initiating and promoting mineral deposition (40). As IBSP, OPN (which is also known as bone sialoprotein1, BSP1) is also considered to be an early marker of bone matrix synthesis, and is associated with initiation of mineralization (41). OCN and ON are reported to be present in fully mineralized matrix and is thus considered as a later marker of osteoblast differentiation. ON is a bone-specific protein that binds selectively to collagen and hydroxyapatite and helps in active mineralization (42). OCN is a final-stage differentiation marker, which is exclusively secreted by mature osteoblasts towards the end of mineralization (43,44). OSX is the downstream mediator for actions of RUNX2 and is considered to be a more specific marker of osteoblasts (45).

Our attempt to understand osteogenic properties of chitosan at a molecular level has revealed interesting findings. This is the first study to show relative fold difference in mRNA levels of hMSCs undergoing osteoblast differentiation on chitosan-coated culture plates. Cells cultured on chitosan-coated plates showed only a slight increase in expression level of *RUNX2*, the gene responsible for osteoblast lineage commitment. However, its downstream effecter OSX had marked increase in expression, specially in initial phases of differentiation. OSX is considered to be the key transcription factor required for differentiation of preosteoblasts to mature osteoblasts (46). Other genes such as *COL1A1*, *ALPL*, *IBSP*, *OPN*, *ON* and *OCN*, which are mostly associated with mineralization, showed several fold increases in levels of expression in cells of chitosan-coated plates. More *COL1A1* expression indicated more calcium binding and thus enhanced mineral matrix deposition on the chitosan-coated plates. Both *IBSP* and *OPN* genes had higher expression in the first week and *COL1A1* and *ALPL* in the second week of differentiation in cells on chitosan-coated plates. Cells on these plates also showed a significant fold difference in expression of *ON* in the second week and *OCN* in the third week of differentiation compared to cells on untreated plates. These findings suggest that chitosan enhances osteoblasts differentiation mainly by upregulating most of the genes associated with calcium binding proteins, which resulted in more bone matrix deposition in cells on chitosan-coated plates. Gene expression profile also indicated that chitosan follows the normal pathway of osteoblast differentiation by human mesenchymal stem cells and embryonic stem cells (47,48).

In conclusion, we report formation of non-adherent, viable and functional cell aggregates by bone marrow-derived hMSCs on chitosan-coated tissue culture plates at higher coating density of chitosan. We also found that hMSCs adhered to the surface of plates with lower coating density of chitosan. In this study, we demonstrated for the first time that chitosan enhanced mineralization by upregulating genes associated with mineralization and calcium-binding proteins. This finding will be useful in designing chitosan-based culture systems for various cell culture and BTE applications. Importantly, our data could be of clinical significance advocating use of chitosan in treating non-union bone fractures.

Acknowledgements

This study was supported by Scientific Council for Industrial Research (CSIR), New Delhi, India.

References

1 Johnell O, Kanis JA (2006) An estimate of the worldwide prevalence and disability associated with osteoporotic fractures. *Osteoporos. Int.* **17**, 1726–1733.

2 Salgado AJ, Coutinho OP, Reis RL (2004) Bone tissue engineering: state of the art and future trends. *Macromol. Biosci.* **4**, 743–765.

3 Kneser U, Schaefer DJ, Polykandriotis E, Horch RE (2006) Tissue engineering of bone: the reconstructive surgeon's point of view. *J. Cell Mol. Med.* **10**, 7–19.

4 Bajada S, Mazakova I, Richardson JB, Ashammakhi N (2008) Updates on stem cells and their applications in regenerative medicine. *J. Tissue Eng. Regen. Med.* **2**, 169–183.

5 Meijer GJ, de Bruijn JD, Koole R, van Blitterswijk CA (2007) Cell-based bone tissue engineering. *PLoS Med.* **4**, e9.

6 Corona BT, Ward CL, Harrison BS, Christ GJ (2010) Regenerative medicine: basic concepts, current status, and future applications. *J. Investig. Med.* **58**, 849–858.

7 Bianco P, Robey PG (2001) Stem cells in tissue engineering. *Nature* **414**, 118–121.

8 Chatterjea A, Meijer G, van Blitterswijk C, de Boer J (2010) Clinical application of human mesenchymal stromal cells for bone tissue engineering. *Stem Cells Int.* **2010**, 215625.

9 Mauney J, Volloch V, Kaplan DL (2005) Role of adult mesenchymal stem cells in bone tissue engineering applications. Current status and future prospects. *Tissue Eng.* **11**, 787–802.

10 Hernandez EC, Mikos AG (2008) New biomaterials as scaffolds for tissue engineering. *Pharm. Res.* **25**, 2345–2347.

11 Meinel L, Karageorgiou V, Fajardo R, Snyder B, Shinde-Patil V, Zichner L *et al.* (2004) Bone tissue engineering using human mesenchymal stem cells: effects of scaffold material and medium flow. *Ann. Biomed. Eng.* **32**, 112–122.

12 Nair LS, Laurencin CT (2006) Polymers as biomaterials for tissue engineering and controlled drug delivery. *Adv. Biochem. Eng. Biotechnol.* **102**, 47–90.

13 Peniche C, Fernández M, Rodríguez G, Parra J, Jimenez J, Bravo AL *et al.* (2007) Cell supports of chitosan/hyaluronic acid and chondroitin sulphate systems. Morphology and biological behaviour. *J. Mater. Sci. Mater. Med.* **18**, 1719–1726.

14 Yang X, Chen X, Wang H (2009) Acceleration of osteogenic differentiation of preosteoblastic cells by chitosan containing nanofibrous scaffolds. *Biomacromolecules* **10**, 2772–2778.

15 Venkatesan J, Kim SK (2010) Chitosan composites for bone tissue engineering – an overview. *Mar. Drugs* **8**, 2252–2266.

16 Pal R, Hanwate M, Totey SM (2008) Effect of holding time, temperature and different parenteral solutions on viability and functionality of adult bone marrow-derived mesenchymal stem cells before transplantation. *J. Tissue Eng. Regen. Med.* **2**, 436–444.

17 Madihally SV, Flake AW, Matthew HT (1999) Maintenance of CD34 expression during proliferation of $CD34^+$ cord blood cells on glycosaminoglycan surfaces. *Stem Cells* **17**, 295–305.

18 Sabokbar A, Millett PJ, Myer B, Rushton N (1994) A rapid, quantitative assay for measuring alkaline phosphatase activity in osteoblastic cells in vitro. *Bone Miner.* **27**, 57–67.

19 Mori K, Shioi A, Jono S, Nishizawa Y, Morii H (1998) Expression of matrix Gla protein (MGP) in an in vitro model of vascular calcification. *FEBS Lett.* **433**, 19–22.

20 Livak KJ, Schmittgen TD (2001) Analysis of relative gene expression data using real-time quantitative pcr and the $2^{-\Delta\Delta CT}$ method. *Methods* **25**, 402–408.

21 Pittenger MF, Mackay AM, Beck SC, Jaiswal RK, Douglas R, Mosca JD *et al.* (1999) Multilineage potential of adult human mesenchymal stem cells. *Science* **284**, 143–147.

22 Caplan AI (1991) Mesenchymal stem cells. *J. Orthop. Res.* **9**, 641–650.

23 Lin SJ, Jee SH, Hsaio WC, Lee SJ, Young TH (2005) Formation of melanocyte spheroids on the chitosan-coated surface. *Biomaterials* **26**, 1413–1422.

24 Clegg RE, Leavesley DI, Pearcy MJ (2005) Mediation of biomaterial–cell interactions by adsorbed proteins: a review. *Tissue Eng.* **11**, 1–18.

25 Hallab NJ, Bundy KJ, O'Connor K, Clark R, Moses RL (1995) Cell adhesion to biomaterials: correlations between surface charge, surface roughness, adsorbed protein, and cell morphology. *J. Long Term Eff. Med. Implants* **5**, 209–231.

26 Chandra V, G S, Phadnis S, Nair PD, Bhonde RR (2009) Generation of pancreatic hormone-expressing islet-like cell aggregates from murine adipose tissue-derived stem cells. *Stem Cells* **27**, 1941–1953.

27 Sila-Asna M, Bunyaratvej A, Maeda S, Kitaguchi H, Bunyaratavej N (2007) Osteoblast differentiation and bone formation gene expression in strontium-inducing bone marrow mesenchymal stem cell. *Kobe J. Med. Sci.* **53**, 25–35.

28 Allen MJ (2003) Biochemical markers of bone metabolism in animals: uses and limitations. *Vet. Clin. Pathol.* **32**, 101–113.

29 Siffert RS (1951) The role of alkaline phosphatase in osteogenesis. *J. Exp. Med.* **93**, 415–426.

30 Golub EE, Boesze-Battaglia K (2007) The role of alkaline phosphatase in mineralization. *Curr. Opin. Orthop.* **18**, 444–448.

31 Balcerzak M, Hamade E, Zhang L, Pikula S, Azzar G, Radisson J *et al.* (2003) The roles of annexins and alkaline phosphatase in mineralization process. *Acta Biochim. Pol.* **50**, 1019–1038.

32 Gong Z, Wezeman FH (2004) Inhibitory effect of alcohol on osteogenic differentiation in human bone marrow-derived mesenchymal stem cells. *Alcohol. Clin. Exp. Res.* **28**, 468–479.

33 Clarke B (2008) Normal bone anatomy and physiology. *Clin. J. Am. Soc. Nephrol.* **3**, S131–S139.

34 Park CJ, Gabrielson NP, Pack DW, Jamison RD, Wagoner Johnson AJ (2009) The effect of chitosan on the migration of neutrophil-like HL60 cells, mediated by IL-8. *Biomaterials* **30**, 436–444.

35 Scanga VI, Goraltchouk A, Nussaiba N, Shoichet MS, Morshead CM (2010) Biomaterials for neural-tissue engineering-chitosan supports the survival, migration, and differentiation of adult-derived neural stem and progenitor cells. *Can. J. Chem.* **88**, 277–287.

36 Fakhry A, Schneider GB, Zaharias R, Senel S (2004) Chitosan supports the initial attachment and spreading of osteoblasts preferentially over fibroblasts. *Biomaterials* **25**, 2075–2079.

37 Komori T (2002) Runx2, a multifunctional transcription factor in skeletal development. *J. Cell. Biochem.* **87**, 1–8.

38 Lian JB, Javed A, Zaidi SK, Lengner CJ, Montecino M, Van Wijnen AJ *et al.* (2004) Regulatory controls for osteoblast growth and differentiation: role of Runx/Cbfa/AML factors. *Crit. Rev. Eukaryot. Gene Expr.* **14**, 1–2.

39 Zhu W, Robey PG, Boskey AL (2009) The regulatory role of matrix proteins in mineralization of bone. In: Marcus R, Feldman D, Nelson D, Rosen CJ, ed. *Fundamentals of Osteoporosis*, pp. 153–202. San Diego, CA: Elsevier Academic Press.

40 Ganss B, Kim RH, Sodek J (1999) Bone sialoprotein. *Crit. Rev. Oral Biol. Med.* **10**, 79–98.

41 Roach HI (1994) Why does bone matrix contain non-collagenous proteins? The possible roles of osteocalcin, osteonectin, osteopontin and bone sialoprotein in bone mineralisation and resorption *Cell Biol. Int.* **18**, 617–628.

42 Termine JD, Kleinman HK, Whitson SW, Conn KM, McGarvey ML, Martin GR (1981) Osteonectin, a bone-specific protein linking mineral to collagen. *Cell* **26**(1 Pt 1): 99–105.

43 Kim GS (1993) Mineralization of bone and osteocalcin gene expression. *J. Oral Biol.* **17**, 101–106.

44 Malaval L, Liu F, Roche P, Aubin JE (1999) Kinetics of osteoprogenitor proliferation and osteoblast differentiation *in vitro*. *J. Cell. Biochem.* **74**, 616–627.

45 Nishio Y, Dong Y, Paris M, O'Keefe RJ, Schwarz EM, Drissi H (2006) Runx2-mediated regulation of the zinc finger Osterix/Sp7 gene. *Gene* **372**, 62–70.

46 Zhang C (2010) Transcriptional regulation of bone formation by the osteoblast-specific transcription factor Osx. *J. Orthop. Surg. Res.* **5**, 37.

47 Kulterer B, Friedl G, Jandrositz A, Sanchez-Cabo F, Prokesch A, Paar C *et al.* (2007) Gene expression profiling of human mesenchymal stem cells derived from bone marrow during expansion and osteoblast differentiation. *BMC Genomics* **8**, 70.

48 Karner E, Unger C, Sloan AJ, Richter LA, Sugars RV, Wendel M (2007) Bone matrix formation in osteogenesis cultures derived from human embryonic stem cells in vitro. *Stem Cells Dev.* **16**, 1–13.